Available online at www.sciencedirect.com
ScienceDirect
Journal of Nuclear Materials 371 (2007) 250–269
journal of nuclear materials
www.elsevier.com/locate/jnucmat

Design challenges for sodium cooled fast reactors

Mamoru Konomura *, Masakazu Ichimiya

Advanced Nuclear System Research and Development Directorate, Japan Atomic Energy Agency, 4002, Narita, O-arai 311-1393, Japan

Abstract

It is of vital importance for commercialized fast reactor to achieve component design with excellent integrity and economics. In the phase II of feasibility study till 2005, a system design for commercialized fast reactor for sodium cooling was achieved. For economical improvement, the system design was undertaken along the guideline including innovative technology for system simplification and new material development. In this paper, the results from the design for shortening of cooling pipings, new components and three dimensional seismic isolation are described, which are design challenges for the sodium cooled fast reactor. Furthermore, in-service inspection and repair is mentioned. Finally, economics for the simplification and the mass reduction employing above technologies are examined.

1. Introduction

A fast reactor (FR) is only energy source which generates its own fuel with sufficient level of safety. No other energy source has this characteristic. But this characteristic would be a weak point from a non-proliferation point of view. Fortunately this will be overcome to utilize minor actinide fuel and proper physical protection system. Then this technology can satisfy the requirement of non-proliferation and safety. On the other hand, economical competitiveness is still issue to be solved. Although technology of a sodium cooled FR has been accomplished up to a demonstration of a nuclear power plant, for example Super-Phenix in France, there is room of technological improvement in order to utilize a sodium cooled FR for commercial use; that is, economical competitiveness should be accomplished. The important points to realize this are the compactness of a sodium cooled FR system taking inspections and repairs into consideration and the increase of reliability of sodium cooling system, which present design challenges for sodium cooled FR.

In this paper, the development of such technologies to achieve economical competitiveness is described. In the following section, our plant design characteristics are described with respect to plant design approach, compactness of sodium cooling system and increasing of reliability of sodium technology. The policy for each issue consists of many innovative technologies.

2. Plant concept

2.1. Overview of plant concept of JSFR

The reactor described here is called JAEA sodium cooled FR (JSFR) [1]. As shown in Fig. 1,

* Corresponding author. Tel.: +81 29 267 7513; fax: +81 29 267 1676.
E-mail addresses: konomura.mamoru@jaea.go.jp (M. Konomura), ichimiya.masakazu@jaea.go.jp (M. Ichimiya).

0022-3115/$ - see front matter © 2007 Elsevier B.V. All rights reserved.
doi:10.1016/j.jnucmat.2007.05.012

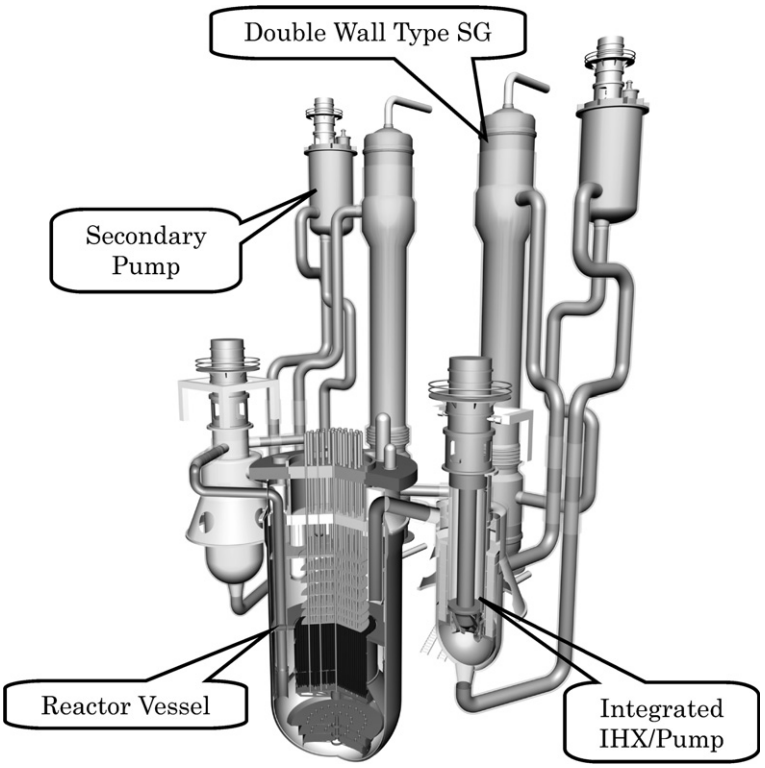

Fig. 1. Plant concept of JSFR.

the reactor is allocated in close proximity to the steam generator (SG) due to shortening of piping. In Fig. 2, a reactor concept of our design has many design improvements. The output power is 1500 MW (electric) with two main loops. The design specifications for JSFR are summarized in Table 1.

A plan figure and an elevation are shown in Figs. 3 and 4. As shown in Fig. 3, the distance between the reactor vessel (RV) and SGs is very short. These main components are set within a space 35.9 m long and 31.8 wide. The primary system (RV and intermediate heat exchanger (IHX)) and secondary system (secondary pump and SG) are set respectively in one area. And this power station has two main reactor systems; that is, it is a twin plant. Each reactor system generates 1500 MWe and the capacity of this station is 3000 MWe. Although the reactors operate independently of each other, they are controlled from one operating room which is shown in the middle above part of Fig. 3.

As shown in Fig. 4, the height of a double walled straight tube typed SG is 37.8 m, which is the tallest component of JSFR. Secondary dump tanks are set in the area under the SG where the secondary sodium system is installed, which is the saving of the building space. As a result, the difference between the center of the IHX and SG is more than enough to induce natural circulation forces. All the components except the SG can be accessed with a polar crane. In case of SG, it will be carried out by a large crane which will be prepared outside of the reactor building. In the right hand side of Fig. 4, the piping layout is shown between IHX and secondary pump. This layout is also very short; however we cannot remove the middle leg pipe of secondary system.

When fuel is exchanged, the spent fuel is pulled out from the core and inserted into an ex-vessel storage tank (EVST) where it is stored in liquid sodium for about one year in order to reduce the decay heat. Then it is pulled out from the EVST and inserted into the water of a spent fuel pool. The time from pulling out from the core to carrying out from the station is four years.

2.2. Overview of plant design approach

In this section, a plant design approach of JSFR is described. In order to achieve economical competitiveness of a sodium cooled FR, the designers can make use of three primary means and their

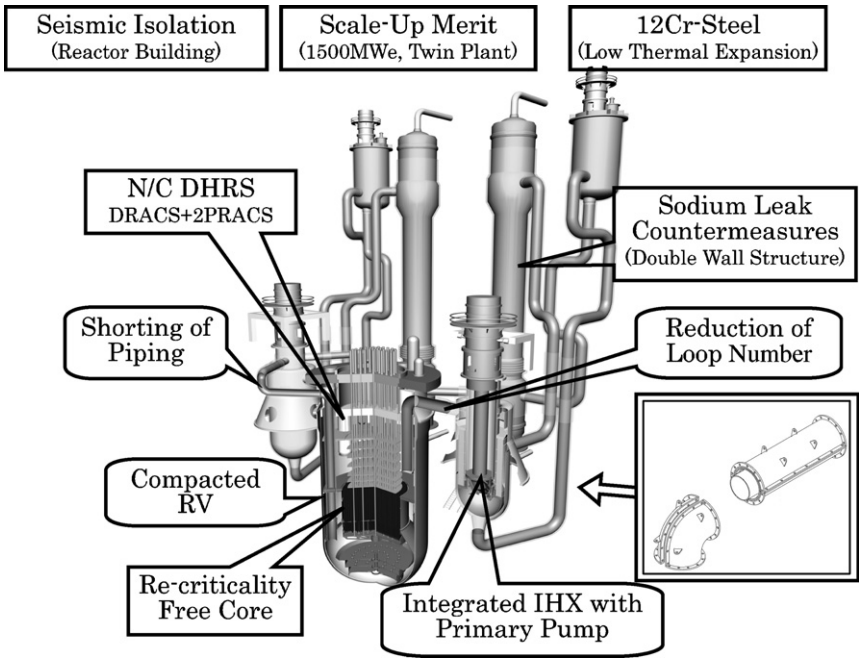

Fig. 2. Design improvements of JSFR.

combination: scale merit, standardization and learning effects, and improvement of design [2]. Scale merit (or economy of scale) is realized the construction cost by increasing the electric output of a reactor. Benefits of standardization and learning effects are realized by reducing construction cost through a mass production with the same standards. Cost reduction is achieved through design by decreasing of the amount of materials for components with innovative technologies which present design challenges compared a conventional design.

In order to achieve compactness with innovative technologies, we look carefully at several physical characteristics of the system configuration: power density of core, flow velocity of coolant, heat transfer coefficient of tubes of heat exchanger and thermal expansion of structural material. Higher power density of core can be achieved with a smaller size of core with the same total power, which allows use of smaller radius reactor vessel. Normally this is one of the most important characteristic of a sodium cooled FR and is achieved by core design.

In a plant design, we turn our attention to the rest of physical characteristics: flow velocity of coolant, heat transfer coefficient of tubes and thermal expansion of structural material. For a given pipe sectional area, higher flow velocity of coolant can reduce the number of loops in a heat transport system, because mass flow rate in a piping is decided by sectional area of pipe, flow velocity and the number of coolant loops. Larger heat transfer coefficient of tubes of heat exchanger can decrease the mass of the tubes and component. Lower thermal expansion of structural material can reduce the number of elbows of piping system, with the result that the volume of reactor building is decreased.

There are two important design points in our plant system. The first point of our design is to realize compactness of sodium cooling system with combination a high sodium flow velocity with reduction of the number of loops and use of ferritic material which has good thermal conductivity and small thermal expansion coefficient. This characteristic makes it possible to reduce the amount of steel mass of a plant, decreasing the construction cost. Furthermore we introduce a complete natural circulation system into the main coolant circuit to operate all electric power supply is out of service, in addition to a decay heat removal circuit, in order to increase reliability of decay heat removal. For this purpose, the coolant pressure drop through the core of JSFR is set lower than the conventional design. As a result, even if a station blackout occurs and all forced power stops, the decay heat can be removed more reliably. This characteristic should be realized by harmony of plant and core design.

The second point of our design is to increase reliability of sodium cooling system, which is related to

Table 1
Design specifications for JSFR

Items		Values
Electricity output (MW)		1500
Reactor vessel	Material	SUS316FR
	Diameter (m)	10.7
	Height (m)	21.2
	Thickness (mm)	30
Piping system	Material	12Cr steel
	Diameter of primary hot leg (HL) (m)	1.2382
	Thickness of primary hot leg (mm)	15.1
	Diameter of primary cold leg (CL) (m)	0.8382
	Thickness of primary cold leg (mm)	12.7
	Outlet temperature of primary coolant (°C)	550
	Inlet temperature of primary coolant (°C)	395
	Outlet temperature of secondary coolant (°C)	520
	Inlet temperature of secondary coolant (°C)	335
IHX	Capacity of an IHX (MW)	1765
	Material of heat transfer tube	12Cr steel
	Length of heat transfer tube (m)	6
	Flow rate of a primary pump (m^3/min)	630
Steam generator	Heat exchange capacity of an SG (MW)	1765
	Material of heat transfer tube	Double wall 12Cr steel
	Temperature of steam (°C)	497
	Pressure of steam (MPa)	19.2
	Temperature of feed water (°C)	240
Turbine efficiency (%)		42.5
Decay heat removal system	Configuration	One direct heat removal auxiliary cooling system Two primary heat removal auxiliary cooling systems
	Capacity of each systems (MW)	23
Spent fuel storage		External vessel storage
Volume of reactor building		151 000 m^3

operational reliance. This is realized with a double-wall concept with a minimum of penetration ports through the outer walls, reducing probability of a leak of coolant sodium from the cooling system to atmosphere. All pipes have their guard pipes and all vessels have their guard vessels. These guard pipes and guard vessels are connected and they make a closed space in which the main pipe is contained. And there is no branch pipe on the main pipe. This design increases toughness against sodium leak from the main pipe. That is, the guard pipes and guard vessels are an engineered safety features system for maintaining a level of sodium in the primary system and retaining any leaked sodium in the gap, if the main pipe were to fail.

An intermediate sodium loop has been set in the conventional design of sodium cooled FR in order to prevent any sodium/water reaction in the SG from leading to core damage. The designers should be allowed an adequate distance between a reactor and a SG for setting this intermediate loop in their design. This distance affects a volume of building of nuclear steam supply system (NSSS) and the amount of mass of structural material of NSSS. The economical competitiveness depends on these values mainly. The characteristics as mentioned above make it possible to reduce a distance between a reactor and a steam generator (SG) with an intermediate sodium loop.

2.3. Design challenges for sodium cooled fast reactor

2.3.1. Compactness of sodium cooling system

For JSFR design, we take six major technologies in order to realize compactness of a sodium cooled

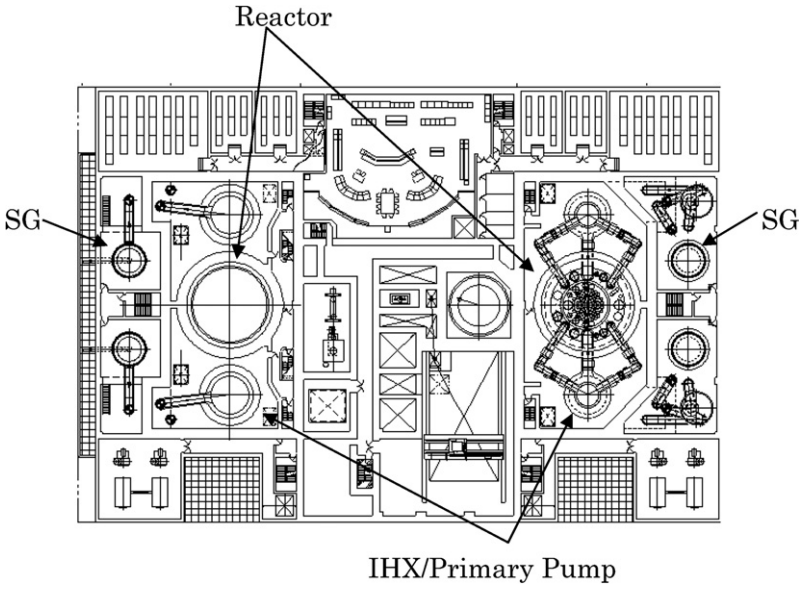

Fig. 3. Plan figure of JSFR.

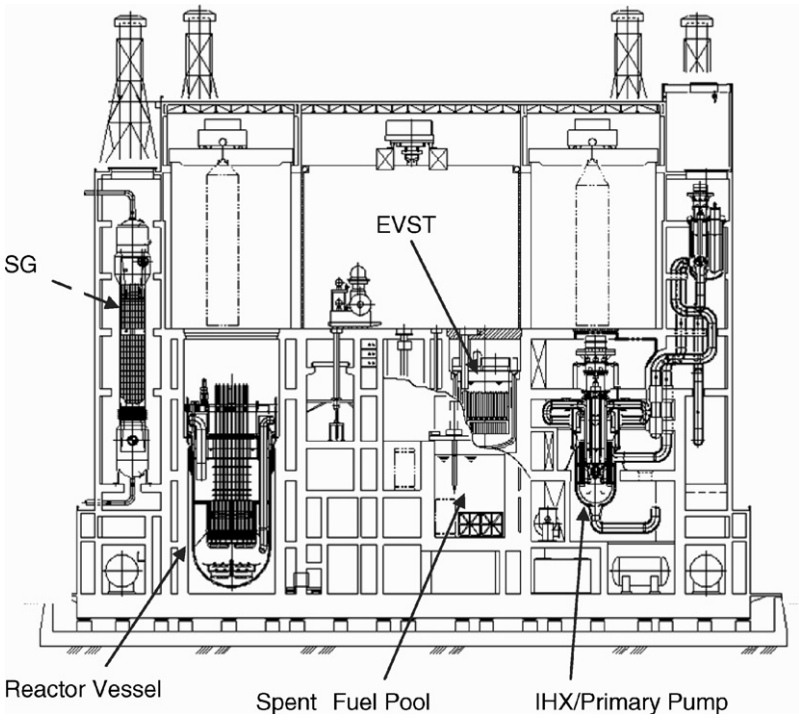

Fig. 4. Elevation of JSFR.

FR as shown in Fig. 2: (1) shortening of piping, (2) reduction of loop number, (3) compact design of reactor structure, (4) integration of components, (5) elevated temperature structural design guide, and (6) seismic isolation technology.

2.3.1.1. Shortening of piping. The shortening of piping and reduction of loop number should be achieved with utilization of ferritic material which has high strength, low thermal expansion and high thermal conductivity, for example 12Cr steel, as shown in

Table 2. Austenitic stainless steels are usually used as structural materials for the primary components of the past and existing sodium cooled FRs, mainly due to their superior elevated temperature strength, ample ductility, and good compatibility with liquid sodium. Since steady and transient thermal stresses, which are displacement controlled in nature, are the primary concern in the structural design, ductile materials are basically preferred. On the contrary, their large thermal expansion characteristics sometimes result in long piping designs with number of elbows. High chromium ferritic steel with optimization of added elements has the capability to improve upon these weak points of austenitic stainless steel. The purpose of using the high Cr ferritic steel is to take a full advantage of its low thermal expansion

Table 2
Comparison of material properties

	Thermal expansion rate (1/K)	Thermal conductivity (W/mK)
Austenitic stainless steel	18.33×10^{-6}	21.75
12Cr steel	13.51×10^{-6}	29.3

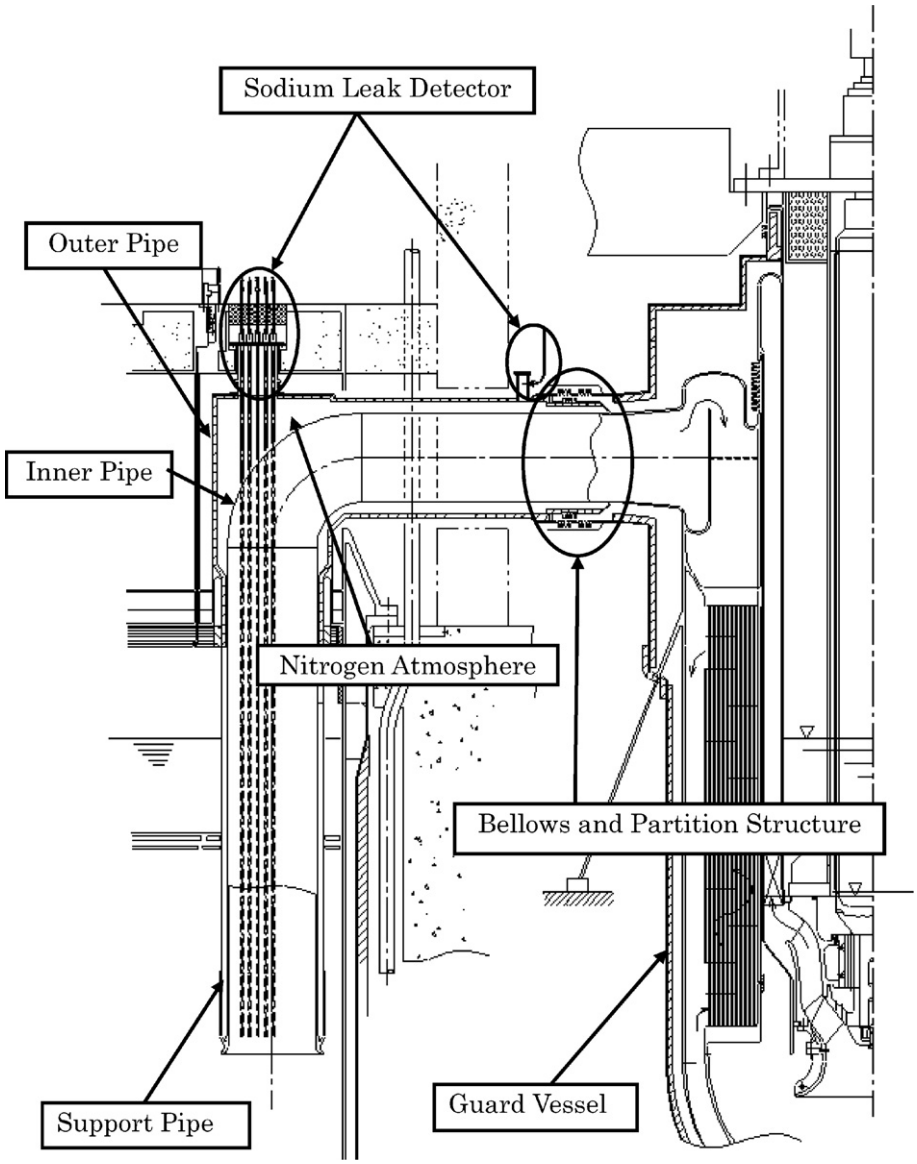

Fig. 5. L-shaped hot leg piping.

and high creep strength in realizing a substantially short primary sodium pipe layout design, which, in turn, leads to a compact components layout and reduces NSSS volume. Each loop consists of one L-shaped hot leg (HL) piping and two cold leg (CL) pipings. In Fig. 5, the L-shaped HL piping is shown. The main pipe is indicated with 'inner pipe' in the figure. The inlet of inner pipe is connected with 'support pipe' which goes down from a roof deck around the inner pipe. The inner pipe on the side of the reactor goes up straight to an elbow, turns to the IHX horizontally and is welded to the outer shell of the IHX with a nozzle. All the inner pipe is covered with outer pipe and the guard vessel of the IHX, that is, double-wall system. The load of the piping is supported at both the connection between the roof deck and the support pipe and the section of the nozzle of IHX shell. The thermal expansion is absorbed with two straight pipes. That is, almost angular deformation is absorbed with these two straight pipes. Such a shortened piping layout with one elbow is realized with the aid of an adoption of ferritic steel which embodies high strength and low thermal expansion coefficient. In this concept, the primary HL piping has been drastically shortened and simplified as shown in Table 3 compared with the Japanese demonstration fast breeder reactor (DFBR: 600 MWe) and Prototype FBR MONJU.

This simple L-shaped short piping design system has different materials: the roof deck is made from usual carbon steel, the support pipe, the inner pipe and the shell of IHX is high Cr steel, and the outer pipe is austenitic stainless steel. Therefore, a dissimilar metal weld cannot be avoided. In this design, such a weld is made at the location which the support pipe is connected to the roof deck, because the temperature at the location is cold: less than around 100 °C. Considering that a remarkable strain concentrates on the primary piping, the stress and strain at the concerned part have been estimated, and it has been shown that the strain (ratcheting deformation) due to repeated thermal stress is not accumulated as high Cr steel is adopted.

The adoption of high Cr steel with high strength and high thermal conductivity makes it possible to enlarge the heat transfer capacity further than that the conventional design because a thinner heat transfer tube is available and it is easier to ensure the structural integrity against thermal stress by a large-sized tube sheet. This allows a design of larger capacity heat exchangers. In the design of the JSFR, the capacity of heat exchanger, that is, the heat transfer capacity per one cooling loop has been enlarged and then the number of loops has been reduced to two loops. As a result, the cooling system has been remarkably simplified.

2.3.1.2. Reduction of loop number. Concerning the reduction of cooling loops, the primary cooling pipings are shown in Fig. 1. The primary cooling pipings perforate the roof deck of the RV. In order to achieve compactness of cooling system, higher coolant velocity should be applied in this design with a reduction in loop numbers. Then larger diameter pipings are applied.

From a hydrodynamic point of view, sodium flow velocity in the primary piping increases up to approximately 9 m/s, and the maximum Reynolds (Re) number of HL piping reaches 4.2×10^7, which is much higher than past sodium cooled FR design conditions. This leads to make a piping design within some limit of a cross section of pipe. And higher sodium flow velocity in pipings with a reduction of loop numbers should be studied carefully. In JSFR, thin piping is adopted because of lower design pressure conditions. Therefore, in the piping design, it is necessary to pay attention to the flow-induced vibration (FIV) of the thin piping under high velocity conditions [3,4]. However, knowledge concerning hydraulic behavior around the elbow and the vibration data of the large diameter piping under high velocity conditions was insufficient. Thus, it is necessary to acquire both hydraulic and FIV data to confirm the structural integrity of the piping system. To solve the above issues, we have performed some water experiments, and the results indicate that the structure should be viable.

In order to clarify the hydraulic and vibration behaviors in the primary cooling pipings, FIV tests were carried out using a water test loop as shown in

Table 3
Comparison of the hot leg piping design

Plant	Design	Material	Outer diameter (mm)	Length (m)	Fluid velocity (m/s)
JSFR	L-shaped top entry	12Cr	1270.0	13.4	9.2
Demo plant	Inverse U-shaped top entry	316FR	965.2	22.3	4.8
Prototype Plant Monju	High piping layout side entry	SUS304	812.8	39	3.5

Fig. 6. The test section simulates HL piping including an elbow of the primary cooling system, which is the largest piping of the JSFR, at 1/3 reduced scale. The test section is set on the top of the rectification tank, which corresponds to the reactor upper plenum. Two types of elbow test pieces can be exchanged according to the test purpose. One is an acrylic pipe to examine the flow pattern and to measure the pressure fluctuations on the piping wall which are the exiting force to the pipe wall. The other is a stainless steel pipe to understand the vibration response. The stiffness of the steel pipe almost agrees with that of the actual HL piping.

Based on test results, we plan to clarify the dependency of velocity or *Re* number on pressure loss and pressure fluctuations on pipe wall in order to extrapolate to designed HL condition. As a first step, we have performed a flow visualization test using an acrylic pipe. In this test, the mean velocity was changed from 0.8 to 9.2 m/s (the same velocity as that of the designed HL piping) by using room temperature water.

The main stream in the piping separated from the inside surface at the corner of the elbow, then it re-attached at about 290 mm downstream from the separated point. Further, the discharge of vortexes was observed intermittently from the region of flow separation to the downstream.

The flow pattern and the velocity profiles in the piping were also examined in lower velocity conditions (0.8 to 7.0 m/s). However, no clear difference in flow pattern and the velocity profiles in the piping were independent of the *Re* number.

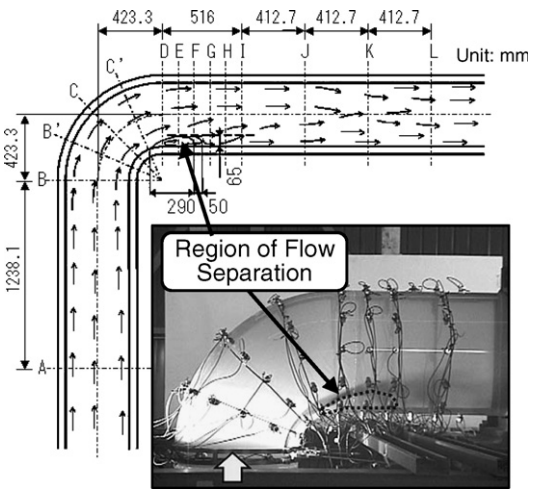

Fig. 6. Visualization in elbow model.

The pressure loss of the piping corresponds to the energy provided by the flow turbulence, so the pressure loss can be used to estimate the intensity of the turbulence in the elbow. In this test, pressure loss coefficient was measured up to 3.7×10^6 of *Re* number, which is one order higher than existing data. In this high *Re* number area, the pressure loss coefficient was in the post-critical regime. This indicated that the turbulence energy given by the elbow was small even in higher *Re* number region [5].

The pressure fluctuations on the piping wall were measured with the pressure sensor installed in the axial and circumferential directions of the elbow model. The experiment shows the spatial distribution of variances of the measured pressure fluctuations at 9.2 m/s of the mean velocity. It was shown that the pressure fluctuation was high in the region of flow separation. The maximum value was indicated at the re-attachment point. As a result, it was confirmed that the behaviors of the pressure fluctuations on the piping greatly changed along the flow direction owing to the turbulence formed in the region of flow separation.

From this large-sized water experiment, the applicability of large-sized piping system to JSFR should be viable from a thermo-hydraulic point of view.

2.3.1.3. Compact design of reactor structure. The compact design of reactor structure should be realized by simplification of the fuel handling system, hot vessel design, seismic isolation and re-criticality free core design. In particular, the hydraulic design of cooling system is essential, and flow optimization in an upper plenum of JSFR is very important. A conceptual drawing of a RV is shown in Fig. 7. The diameter of the RV is reduced by adopting a compact core design and a single rotating plug, combined with a simplified manipulator-type fuel handling machine (FHM). In the upper plenum region, various structures are arranged: HL and CL pipes of the primary cooling system, double dipped plates (D/Ps) for prevention of cover gas entrainment, a decay heat exchanger for a decay heat removal system, two cold traps for a sodium purification system, and a shell-less column type upper internal structure (UIS). In order to manage flow configuration of sodium, the UIS consists of the combination of six perforated plates and control rod guide tubes (called column-type UIS).

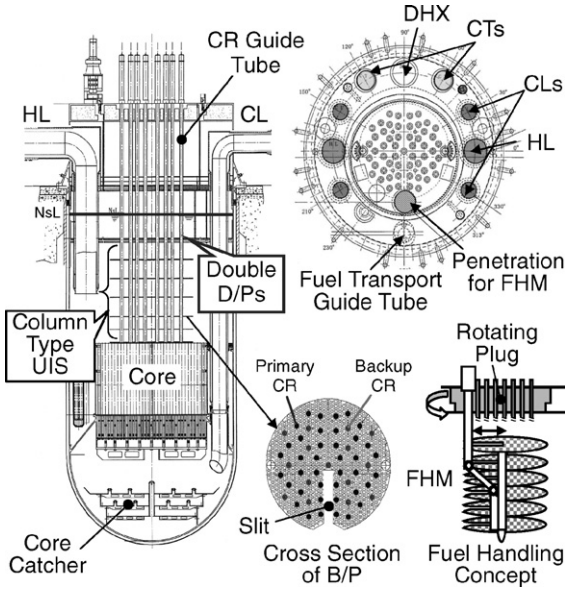

Fig. 7. Conceptual drawing of RV.

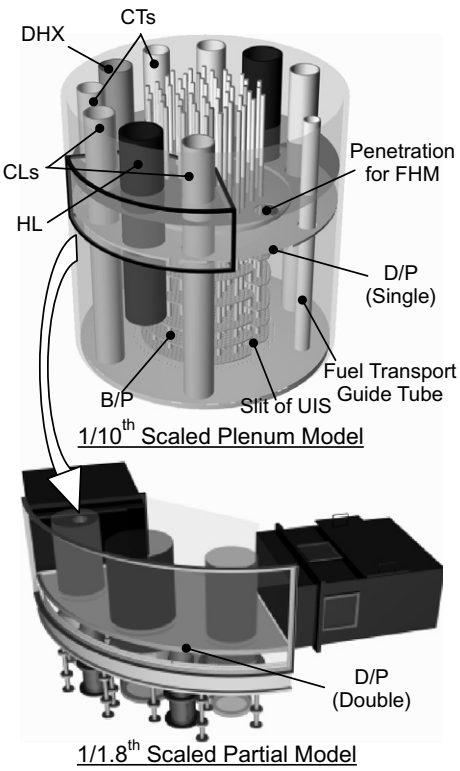

Fig. 8. Test models for upper plenum.

Therefore, sodium that flows out from the core outlet rises inside the UIS through these plates. All of these plates have radial slits in order to pass through the arm of the FHM toward the core center. This slit of UIS causes very complicated flow pattern in an upper plenum.

Electric output of JSFR is 2.5 times greater than that of the DFBR, though the size of the RV is nearly the same as the DFBR. By adopting the compacted RV, the sodium mass flow rate in the RV is thus 2.5 times higher than that in the DFBR. Further, it is predicted that a high velocity upward flow is formed through the UIS slit and that this upward flow collides directly with the D/Ps. Under this complicated flow field, potential of gas entrainment at the free surface would be increased. Therefore, it is necessary to clarify the flow pattern in the upper plenum and to confirm the effectiveness of the D/Ps with respect to the prevention of gas entrainment. We have performed several water experiments and proposed a design solution of the structure of the upper plenum.

Two types of water experiments [6,7] have been performed in order to clarify the flow pattern in the upper plenum. One is a 1/10th scaled plenum model which simulates the entire region of the actual plenum in order to confirm the flow pattern. The other is 1/1.8th scaled partial model shown in Fig. 8, which simulates a 90-degree sector of the upper region above the D/Ps in order to evaluate the scale effect of the test models and the onset conditions of the gas entrainment.

At first, the flow pattern with the 1/10th plenum model was examined in two conditions. One is the Froude (Fr) number similar condition where free surface deformation and also the flow pattern are expected to be similar to that in the designed reactor. The other has the same velocity conditions as the reactor which is set as a criterion to examine the onset conditions of gas entrainment based on the similarity study for DFBR [8].

In the case of the Fr number similar conditions, the free surface was relatively smooth. In the case of same velocity conditions, the upward flow through the gap between the D/P and RV wall reached the free surface and lifted up the free surface, but no gas entrainment was observed. These results showed that the D/P was effective to prevent gas entrainment even in same velocity condition. However, it was clarified that a countermeasure to suppress the upward flow through the D/P gap in front of the UIS slit was necessary.

As another issue, vortex cavitations were found near the HL intake: one was stretched from the RV wall and the other two were from both CLs.

It was considered that these vortex cavitations were mainly caused by high velocity rotating flow sucked into the HL. In general, cavitations formed in the fluid machinery have the potential to damage the components, so the countermeasure to suppress the vortex cavitation was also necessary to maintain the structural integrity for piping.

As countermeasures for flow optimization, two flow control devices were proposed from the experiments [6]. As shown in Fig. 9, one is an FHM plug, which is a cylinder inserted in the penetration for the FHM during the normal operation period in order to suppress upward flow from the UIS slit. The other is a flow splitter which is set on the RV wall facing the HL piping to control the vortex cavitation stretched from the RV wall. A triangular pillar type of vertical rib has been adopted as one of the devices to prevent the vortex cavitation in pump sumps. These devices were effective to flow optimization from experiments, and were introduced in the reactor design.

Furthermore, concerning to the scale effect on the gas entrainment, another water test experiment was performed using the 1/1.8th scaled partial model as shown in Fig. 8. Rated condition of the circumferential velocity (V_c) and downward flow velocity through the gap of the D/P (V_g) were estimated as the condition in the designed reactor based on the measured velocity profiles in the 1/10th scaled full sector model. As shown in Fig. 10, it was found that the circumferential velocity was the dominant factor on the onset condition of gas entrainment, and the downward velocity through the D/P gaps was less effective in the case of high water level condition [7]. Based on the test results, it was clarified that the present D/P design had enough margins to prevent the gas entrainment.

A computational fluid dynamics (CFD) analysis was performed in the designed reactor geometry.

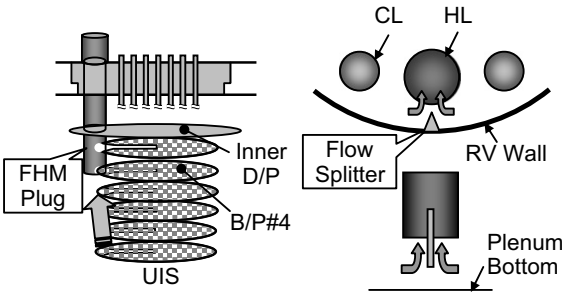

Fig. 9. Flow control devices.

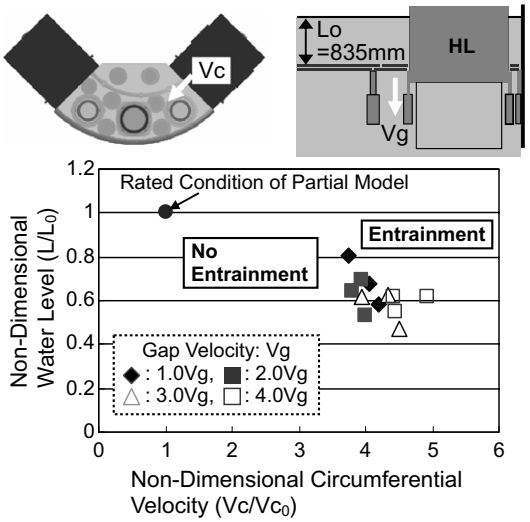

Fig. 10. Map for onset condition of gas entrainment.

The flow pattern near the FHM plug was in good agreement with velocity field measured by particle image velocimetry in the 1/10th plenum model. The maximum velocity at free surface in the RV was approximately 0.1 m/s [3]. Maximum surface velocity of 0.1 m/s or less was provided as a criterion for prevention of gas entrainment based on the DFBR test results. From this analytical result, we have prospected that the gas entrainment could be prevented by applying the flow splitters which are set up on the louver-shaped thermal liner facing both HL pipes.

Based on the results of water experiments and the CFD analysis, flow field in the upper plenum was optimized by applying D/Ps and flow control devices.

So the management of the upper plenum with a high sodium velocity can be found, which would be viable on a concept of a compact RV and a UIS without outer shell.

2.3.1.4. Integration of components. An 'integrated pump/IHX component' is also selected for JSFR primary cooling system. This component design aims at compactness of cooling system and improvement of maintenance capability. The integration of components can be achieved by installing a primary pump into an IHX with a common vessel. Therefore the primary cooling system is composed of only three main vessels: a reactor vessel and two integration component vessels. Although the integration component leads to a larger tube sheet

diameter of the IHX, the utilization of high Cr steel ensures structural integrity as previously mentioned due to the characteristics of this material.

As shown in Fig. 11, the integrated pump/IHX component consists of homocentric pump and IHX in one vessel. To increase heat exchange capability, baffle plates are installed and they support the tube bundle with 0.1–0.3 mm gaps. In this component, a pump shaft does not have enough cross section to keep stiffness for its own vibration frequency and heat transfer tube is weak structure for vibration and detrition with the baffle plate. For the tube integrity, vibration transfer from pump shaft to tubes is maintained at a low value throughout the 60-year operating period. This vibration control design is a key technology for the integrated pump/IHX component.

The final goal of the component design is 'design by analysis' and the next two issues should be developed for it. (1) Vibration transfer from pump shaft to heat transfer tube should be maintained sufficiently low. For the vibration controlled design, analysis method on vibration transfer in the structure is important issue. (2) Wear-out behavior on heat transfer tube should be investigated, because heat transfer tubes are made from a new material, that is, high Cr steel. For the reliable design, wear-out data is needed.

To develop vibration transfer controlled design, scale model experiment and analytical studies were carried out. In order to establish its design feasibility and to develop a methods of vibration control design, 1/4 scaled experiment has been carried out [9]. An inertial vibration exciter was placed in a simulated pump casing of test apparatus and the exciter generated vibration. The frequency response characteristic was acquired from a result of data analysis. The analysis was done using 3D shell model of FINAS code, which was developed by JAEA and has a fluid structure interaction module and can directly handle the vibration behavior of complex multi-cylinders with fluid between the cylinders, and the analytical results were compared with the test results.

Using the evaluation method which is developed by 1/4 scale experiment and analysis, the component design is evaluated. It is evaluated that there is no resonant frequency vibration mode for pump speeds of 100% operation, 44% (initial low power operation), and 10% (stand by) with safety margin 20%. Then the component design is evaluated as feasible.

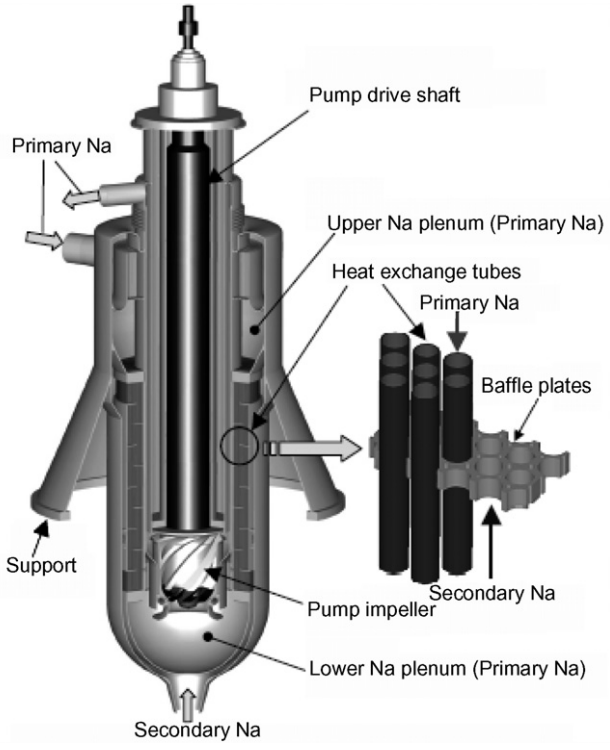

Fig. 11. Structure of the integrated IHX/pump component.

In the future work, 1/4 scaled experiment using mechanical pump and the wear-out experiment on heat transfer tube are planned. From these experiments, the design evaluation method will have enough accuracy to assure the integrity of tube and component for the operating period.

2.3.1.5. Elevated temperature structural design guide. Particular characteristics of structural design of a sodium cooled FR are low pressure and high temperature conditions due to the use of liquid metal as a coolant. Under a high temperature condition, the thermal stress induced by the temperature difference in the structure increases; further, elastic, plastic and creep deformation easily occur due to a decrease in the yield strength of the material. Therefore, elevated temperature structural design methods are required for assuring structural integrity under above conditions. For that reason we have prepared an elevated temperature structural design guide.

The first established sodium cooled FR structural design code in Japan was the 'elevated temperature structural design guide for class 1 components of prototype fast breeder reactor (ETSDG for prototype) [10]' which was developed by extension of the ASME B&PV Code Sec. III CC1592 [11]. Introducing additional developments of materials and structural analysis methods to ETSDG for prototype, the 'elevated temperature structural design guide for demonstration fast breeder reactor (ETSDG for DFBR) [12]' was developed.

Furthermore, commercialized FRs have different design needs from prototype and DFBR. To satisfy above needs, new design methods are developed and integrated with ETSDG for DFBR into ETSDG for commercialized FR with two sets of guidelines for inelastic design analysis and for thermal load modeling [13].

Consider the compact and simple plant design of the JSFR as shown in Fig. 2. Removal of protection equipments for the reactor vessel wall (reactor wall cooling system, etc.) increases the thermal stress on the relevant section. Further, in a small, thin-walled vessel, the primary stress for supporting the core weight overlaid on the reactor vessel wall becomes larger than that observed in previous FRs. These loading conditions enhance ratchet deformation and (creep) fatigue damage at a vessel wall around liquid free surface and at a lower part of vessel.

With regard to the cooling system, the decrease of an amount of coolant and the high coolant flow velocity cause a severe thermal transient load. It increases risk of high cycle thermal fatigue of pipes which is typical problem at mixing zone of high and low temperature fluid.

In order to overcome the above structural design problems, ETSDG for commercialized FR introduces several new technologies. (1) Some severe parts of reactor vessel and IHX are located in the cold leg where normal operating temperature is under creep regime. To treat these parts as non-creep design area, classification method of high temperature design area is improved. (2) When both ratchet strain and fatigue damages increase, there is a possibility of those interactions. Failure criteria considering those interactions are investigated. (3) To predict inelastic response of structures, inelastic constitutive equations and (4) design evaluation method based on inelastic analysis results are recommended [14]. In spite of more severe thermal loads, conventional design guides for FRs have no rule for thermal load modeling. (5) Load modeling methods are studied for system thermal transient load [15] and (6) thermal striping load [16,17].

Above developments are integrated with ETSDG for DFBR into ETSDG for commercialized FR which consists of 'elevated temperature structural design guide', 'guidelines for inelastic design analysis' and 'guidelines for thermal load modeling'.

2.3.1.6. Three-dimensional seismic isolation technology. Sodium cooled FR components adopt thin wall structures since their low constraint conditions are advantageous to mitigation of thermal stresses. Additionally, a low pressure condition dose not require a thick wall. However, flexible structures have disadvantage against seismic load. In order to reconcile opposite requirements from thermal and seismic loads, seismic isolation technology would be desired.

In the design of JSFR, many innovative technologies are introduced, which requires sophistication of the mitigation of seismic loads. Two types of three-dimensional seismic isolation systems for FR are developed in the R&D project from the viewpoints of realization and economic competency [18]. One is a three-dimensional, entire-building seismic isolation system (3D-SIS) and the other is a vertical isolation of main components with horizontal base isolation system (Vertical+2D-SIS), which are schematically shown in Fig. 12. 3D-SIS supports the entire reactor building as shown in Fig. 12(a). As for the Vertical+2D-SIS, horizontal seismic

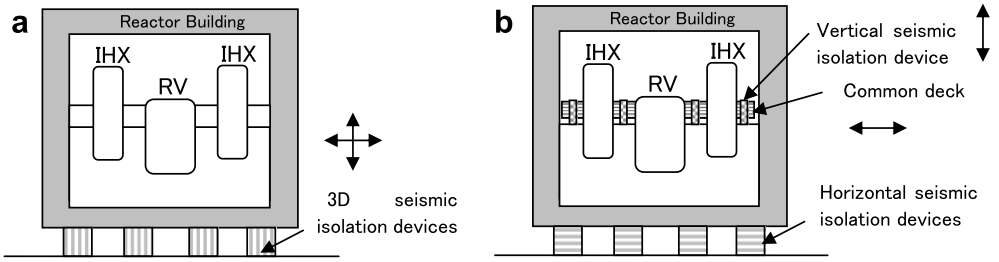

Fig. 12. Three-dimensional seismic isolation systems.

isolation devices support the reactor building and vertical seismic isolation devices support 'common deck' that holds main components such as RV, IHX as shown in Fig. 12(b).

As for 3D-SIS, 'rolling seal (U-shape rubber) type air spring' is adopted as its device. At the same time, 'hydraulic type of rocking suppression cylinder system' is added to suppress the excessive rocking motions of the building, which occurs in the three-dimensional isolated structure. The reactor building weighs about 2700 MN, and target performance of the system is that the natural period is greater than or equal to 1.0 s and the damping ratio is more than 0.2. Air springs (160) are placed around the inner area and 112 hydraulic supports function with rocking suppression systems around the outer area. Hydraulic pressure of the load support cylinder is transferred to rocking suppression cylinder and further to an accumulator unit which mitigates the shock of the vertical load by a bladder inside. All piston rods of the rocking suppression cylinder are connected each other to suppress the entire rocking motion.

As for Vertical+2D-SIS, a reactor vessel and major primary components are suspended from a large common deck supported by vertical isolation devices consisting of large coned disk springs and steel beam dampers. The isolation device, which can achieve vertical isolation frequency of 1 Hz and damping ratio of 20%, is designed. The device is composed of 70 coned disk springs of 1 m outside diameter. The damper is made to be a tapering beam damper so that the stress distribution may become uniform. The applicability of the common deck isolation system to a sodium cooled loop type FR plant is examined. Total installation weight is about 6000 ton, and it is supported by 20 isolation devices. Considering weight distribution and rigidity allocation, the isolation device is mainly placed at the circumference of the reactor vessel and peripheral part of the deck. Horizontal load support structure is established so as not to exert the horizontal load on the vertical isolation device. Full scale coned disk spring and damper performance tests were carried, and the validity of design methods was confirmed. A series of shaking table tests using a 1/8 scale model was performed. As a result, it is confirmed that proposed isolation system is quite effective in mitigating seismic loads to major components.

2.3.2. Increasing of reliability of sodium system

2.3.2.1. Countermeasures against the chemical potential of sodium (double-wall concept). It is important to increase reliability of sodium system in order to attain economical competitiveness of a sodium cooled FR system and to keep a high load factor. For this purpose, a double-wall concept is adopted in this design. All main pipes and vessels have each guard pipes and guard vessels which are connected and make a closed area with nitrogen atmosphere. If a defect occurs at a main pipe and sodium coolant leaks from a crack, the guard pipe will keep the leaked sodium in the annular space between main and guard pipe, then the leaked sodium will not be exposed to air. In this double-wall concept, a sodium boundary is set at the main piping and main vessels, that is, the inner wall. The function of outer wall is to contain sodium during an accident condition in which the sodium mass flow rate is quite less than the full power condition.

As for the primary system, the guard pipe and guard vessel are airproof and sodium leakage is restricted. And sodium combustion is prevented because the closed space inside the outer wall has inert atmosphere filled with nitrogen gas. Therefore, welding structure is adopted for outer wall because of the requirement of leak-tightness for sodium. The countermeasures to sodium leakage at primary piping is shown in Fig. 5.

As for the secondary system, the space inside the enclosure of sodium pipe and components also have

inert atmosphere because of restriction for sodium combustion. As the secondary system is not a safety system and leak-tightness is not required for enclosure, a lip-seal structure is adopted for the enclosure flange as shown in Fig. 2. Therefore, repair capability is improved and the recovery time after a sodium leak is shortened.

We make a design of a part of penetration through the double-wall with great care. The number of such parts in the cooling system should be minimized. For example, in the conventional design, an electromagnetic flow meter is utilized as a coolant flow meter. But a ferritic material in our design has magnetic characteristic under which an electromagnetic flow meter cannot work well. Then we pick up an ultrasonic flow meter technology which need not pierce the double-wall. And this flow meter can be utilized also as a thermometer which need not pierce the walls as would a conventional thermometer.

Furthermore, the frequency of sodium leak is reduced because the area of sodium boundary is reduced by elimination of branch pipes from main pipe of primary and secondary cooling system.

Partition structure is adopted in the annular space between main and guard pipe. Then, the increment of leaked sodium and the aerosol diffusion is limited by these partitions and it is easier to locate and recover the leaked region. However, a large number of partitions make it difficult to construct piping systems. Therefore there is a good balance of localization and construction.

2.3.2.2. Double wall straight tube steam generator. It is desirable that sodium heated SGs of a commercialized FR should avoid the possibility of sodium/water reaction, because the failure of plural heat transfer tubes by reaction jets or reaction products significantly affects the operating time of the plant, that is, which can reduce operating revenue and increase operating cost.

Then, a double-wall type that consists of inner and outer tubes is employed for heat transfer tubes of an SG in order to prevent sodium/water reaction practically [19,20]. The conceptual picture of a double-wall tube SG is shown in Fig. 13. Both tubes are mechanically contacted by pre-stress, and they are fabricated in straight type. The integrity of inner and outer tubes is confirmed by ultrasonic test (UT) and eddy current test (ECT) during the periodic inspection of the plant. These tube examinations are necessary to prevent simultaneous failure of the inner and outer tubes.

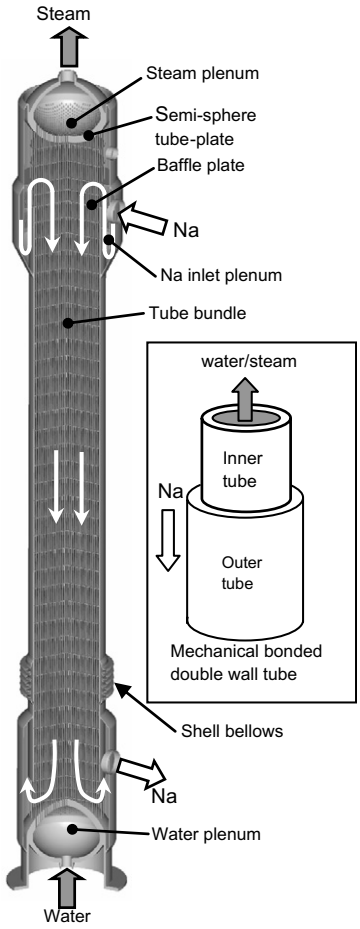

Fig. 13. Double wall straight tube steam generator.

As for the heat transfer performance for double-wall tube, sufficient pre-stress of the interface between inner and outer tubes can avoid thermal deteriorations in the duration of service (60 years) without being affected by interface stress relaxations. This was shown by our analysis [21].

Since the heat exchange capacity of the SG of JSFR is very large for enhancing cost-effectiveness by scale merit, the diameter of the SG shell is also large. Therefore, the shape of tube sheet is semi-sphere type standing for the water-side pressure. Besides, this tube sheet is single type to simplify its structure and plugging process.

From the thermal-hydraulic perspective, the down and up flow of sodium by baffle plate structure which surrounds a sodium inlet plenum of the SG can unify the radius sodium flow distribution into the tube bundle region seen in Fig. 13. This uniform sodium flow contributes to flatten a horizontal temperature distribution in the bundle

region. This is indispensable for preventing a tube buckling or tube-to-tube sheet junction failure. The shell bellows can compensate the thermal expansion difference between the SG shell and the tube bundle.

Sodium and water flow is counter-flow, and the sodium flow parallels the tubes of SG in order to reduce the pressure loss and to avoid tube-fretting. No flow dynamic instability in water side occurs by increasing water pressure without orifice [20]. This orifice-less method helps the tube reliability in terms of undesirable phenomena like erosion or blockage at the orifice.

2.3.2.3. Development of in-service inspection and repair. From early stage of the design, many concepts for inspection and repairing mechanism are incorporated into the JSFR design. The design policy of in-service inspection (ISI) is that every part can be looked at whenever one wants to and several parts can be repaired when necessary.

Sodium is an opaque medium and an object in sodium fluid cannot be seen directly. Furthermore sodium is chemically active. These characteristics are a weak point of a sodium cooled FR from inspecting and repairing point of view. Although the most important point in a design of a sodium cooled FR should be to attain high reliability, the inspection and repair technologies are key issues for commercialization of a sodium cooled FR. When the inspection and the repair are examined, we should consider the double-wall structure from leakage point of view and the reducing atmosphere in sodium from corrosion point of view. Assuming that all the functions of each component for safety are maintained, reasonable inspection method considering the above characteristics of a sodium cooled FR system should be established with respect to ISI. For example, for core support structures, only the defect check should be needed to assure that there is enough tolerance against a structural deformation, because the structure exists in low pressure difference circumstance.

Continuous leakage monitors can detect a small leakage at coolant boundary in its early stage in order to maintain a reactor core cooling function. Even if a leak occurs, the reactor core cooling function can be maintained with double-wall concept: a guard vessel and guard pipes. To assure the intactness of the double-wall concept, a guard vessel and guard pipes should be checked with VTM-1 or a leak rate examination which confirms that no penetration defect is generated.

The monitoring devices for visualization with high resolution and the device for volume examination should be developed in order to perform a visual examination for these structures inside the reactor vessel.

Although the SG in our design is not expected for the safety function of decay heat removal during an accident, a water leak rate of a failed heating tube should be limited in order to keep intactness of coolant boundary, early restart and preservation of property. So, ISI should confirm the integrity of heating tubes, tube sheets, baffle plates and welding points. Several R&D activities have been performed in this field: ultrasonic device for camera, treatment of cables and device moving in sodium.

The design of JSFR includes the way to inspect and to repair, especially a reactor structure, an integrated pump/IHX and an SG. For example, there is an inspection hole between each main heat transport pipe in a RV. And this inspection hole goes from a top of the roof deck through the reactor core support skirt. The four inspection holes in total should be needed to access the range around all the reactor core support skirt and the lower plenum.

The method of the localization of a damaged position is examined for the primary system pipe, the secondary system pipe, and the IHX heat exchanger tube. After the damaged section is roughly specified by the signal of the leakage detector, the damage position is visually identified by the fiberscope for the primary piping system. Therefore, for the primary piping system, the guide of the fiberscope is set beforehand on the inside of the outer pipe. On the contrary, for the secondary piping system, the damage position is identified by direct removing outer pipe. For the secondary piping system, the gap of inner and outer pipe is divided into independent sections in order to identify a damaged section by each individual leakage detector. In addition, the outer pipe has a flange structure in order to remove it easily as shown in Fig. 2.

For repairing methods, we classified repairing issues into three categories according to the frequency of the damage. The first category is that there is a possibility of occurrence of damage in a plant-life time, for example a loosened bolt of dipped plate. And it is assured in this category that the repair should be performed easily in short time. The second category is that the possibility is lower than the first category, for example a crack of

primary main pipe. And it is assured in this category that the repair should be performed even if it takes longer time. The last category is that the possibility is extremely very low. The decision of repair would be expected by plant owner on a case-by-case basis.

If the draining of sodium is needed at the repair, it requires a long-duration procedure, especially for large-sized components such as RV and SG. Therefore it is desired that repairing is performed without coolant draining as long as possible for shortening of inspection period and improvement of availability. Consequently, development of repairing technologies which can be implemented under the circumstance of high temperature and high radiation is needed. Such technologies in sodium coolant are also required for the structures in reactor vessel such as core support structure. So there are many development issues as follows: information of wetting effect of ultrasonic transducer, development of ultrasonic transducer resistant to high temperature, high resolution image processing program, phased array ultrasonic system, and so on. And the method to carry the equipment to the examination parts must also be developed.

2.3.3. Other important design topics

A thermal source for hydrogen production is an attractive utilization of an FR. Hydrogen is noticed to be an energy carrier for next generation and hydrogen fuel cells can be used for both stationary electric generation and transportation. In Japan, a large amount of petroleum is used for transportation and the share of oil imports is above 95% and carbon dioxide emission form transport is increasing. It is desired that the dependence on petroleum should be reduced concerning energy security and environmental protection [22]. Diverse utilization of hydrogen as energy carrier and energy source for transportation can reduce carbon dioxide emission. Nuclear energy is one of the attractive energy sources to produce hydrogen suitable for energy security and reduction of carbon dioxide emission.

A sodium cooled FR can supply heat around 500 °C. There are two hydrogen production methods using sodium cooled FRs. One is the steam reforming at the temperature 500 °C. The other is a steam methane reforming which is still attractive as a low cost hydrogen production method, though the goal of hydrogen production is water splitting without any fossil fuel. And the system design of a steam reforming hydrogen production plant using a sodium cooled FR is studied [23].

Thermochemical and electrolytic hybrid cycle is a new process developed by Nakagiri [24]. The process is based on the Westinghouse process [25] which requires high temperature over 800 °C to decomposition sulfur trioxide gas into sulfur dioxide and oxygen. The new process can be operated at the temperature approximately 500 °C because sulfuric trioxide gas is decomposed by electrolysis with ionic oxygen conductive solid electrolyte such as yttria stabilized ziruconia. The other electrolysis which is also adopted by the Westinghouse process is the room temperature electrolysis of sulfur dioxide solution with polymer electrolyte. Hydrogen production plant with the thermochemical and electrolytic hybrid method using a sodium cooled FR is designed [26]. The ideal hydrogen production efficiency 42% (high heating value) is expected with the thermochemical and electrolytic hybrid cycle, assuming development of high efficiency electrolysis in future.

Hydrogen production system is designed to utilize components of steels such as high Si cast iron, which has good toughness against sulfuric acid. From structural material point of view, prolongation of life time of such structure under very severe acid condition is essential for commercialization.

Hydrogen production with a sodium cooled FR is attractive as a long term energy source with breeding of nuclear fuel. This is coming from some possibilities to use a sodium cooled FR for heat source. The combination of a sodium cooled FR and this method can produce hydrogen, and will convert nuclear energy to chemical energy. For realizing this technology, structural material development should be necessary as mentioned above.

3. High chromium ferritic steel for primary sodium components and pipes

For the shortening of piping and reduction of loop number, a challenge is made to adopt a high chromium ferritic steel, in place of an austenitic stainless steel, to the primary components and pipes except for the reactor vessel. The underlying recognition in this challenge was that, thanks to the advances in the steel production technology, ferritic steels could be used as the structural material of the primary sodium components and high chromium pipes with reliance. In fact, high chromium steels with improved creep strength and weldability were developed for fossil power plant applications. Forging steel (12%Cr) was realized by some major

technical breakthroughs that took place in 1990s, including the technology of eliminating gaseous elements from the steel [27] and the knowledge about the effect of tungsten/molybdenum to the improvement of the high temperature strength [28].

In Fig. 14, the thermal stress resistance of various steels is compared, in which the ordinate is taken as a ratio of creep strength to the thermal stress induced by a certain amount of temperature variation. Here, P122 is a 12%Cr steel originally developed for fossil plant applications. One can note that the 12%Cr steel is somewhat superior to 316FR in terms of this parameter. This superiority of the 12%Cr against thermal stresses comes from its low thermal expansion property and sufficient creep strength. Since the most important property required to JSFR structural materials is the resistance to steady and transient thermal stresses, high Cr steels have a potential as a JSFR structural material.

Structural materials for JSFR components are required to have good performance also in other properties. These include high creep–fatigue strength, sufficient tensile and creep ductility, sufficient fracture toughness, and good weldability.

The major concern on the existing 12%Cr steel for JSFR applications were its low ductility and fracture toughness especially after long aging exposure. Therefore it was judged a sort of optimization of the alloy was inevitable to improve these important properties for the operating condition of JSFR, that is, temperature range of around 550 °C and long operation of 60 years.

The optimum total content of tungsten (W) and molybdenum (Mo) for high Cr steel had been known to be 1.5 wt% as an equivalent Mo content for the improvement of high temperature strength [29]. Empirical knowledge in the steel manufacture was that W had an improving effect on the creep strength of Cr steel at temperatures higher than 600 °C and that Mo was effective at lower temperatures.

A series of long term material tests were run to assess the effects of the W and Mo contents on the creep ductility. Fig. 15 shows the creep reduction of area of three kinds of 12%Cr steels with various W/Mo contents at 550 °C. Data of Mod.9Cr–1Mo steel, whose creep ductility and creep–fatigue strength were the targets of the optimized high Cr steel, are over plotted as a reference. While the creep ductility data of P122 with high W content is inferior to those of other steels, those of the W-free steel falls in the lower scattering band of the data of Mod.9Cr–1Mo steel. Although the number of data is limited, the figure suggests a correlation between the creep ductility and the W content. The results of creep–fatigue tests with one hour dwell at peak tensile strain at 550 °C on these steels showed that at lower strain range, creep–fatigue strength of W-free steel was also superior to those of the other steels. This tendency is consistent with the observation on the creep ductility shown in Fig. 15.

Another important material property is fracture toughness, which is closely related with the leak before break (LBB) characteristics of components

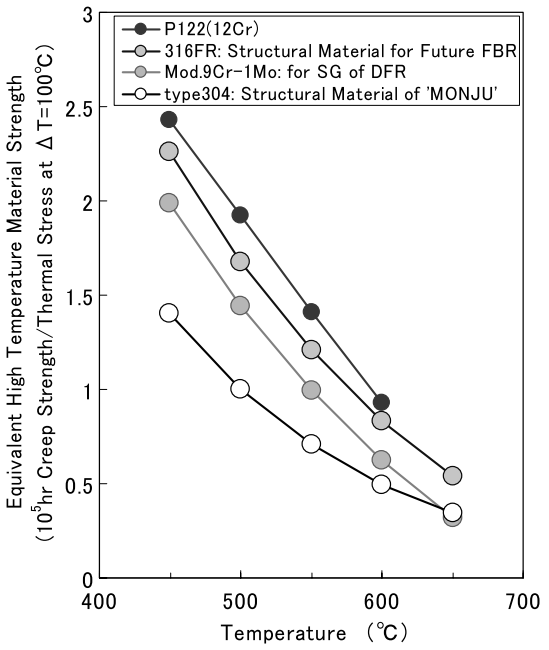

Fig. 14. Comparison of resistivity of some steels for thermal transient loading.

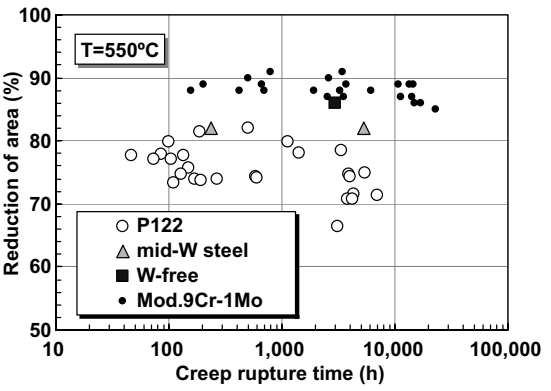

Fig. 15. Creep reduction of area.

and pipes. It was found that the W/Mo content plays a key role here also. As is shown in Fig. 14, the Charpy impact tests results on these high Cr steels before and after aging at 600 °C for 6000 h, which is closely correlated to the fracture toughness, revealed that the upper shelf energies (USE) of the three 12%Cr steels were lower than that of Mod.9Cr–1Mo steel both before and after aging. Among these 12%Cr steels, the USE of P122 with high W content significantly decreased after aging in comparison with those of med.-W content and W-free steels. Based on this observation, an adverse effect of the W content on the fracture toughness after aging was clarified.

A scanning electron microscope (SEM) observation of some aged (600 °C–6000 h) materials revealed the formation of Laves phase, Fe_2W or Fe_2Mo. The amount of Laves phase observed in aged P122 was considerably larger than those of other 12%Cr steels, which coincides with the impact tests results; W tends to form Laves phases more easily than Mo during aging and degrades fracture toughness as a result. Since the stability of the microstructure/metallurgical phase is of a great importance for long term operation at elevated temperatures, this result also suggests the necessity of limiting or eliminating the W content in the optimized alloy.

Ferritic steels have attractive characteristics from a cost-reduction point of view. By now, several material experiments have been done. And the possibility to apply a sodium cooled FR would be found; that is, the resistance to thermal stress of ferritic steel could be achieved by the optimization of several elements in ferritic steel, although the more experiments are required on several conditions (temperature, stress, etc.) in order to confirm applicability for a sodium cooled FR.

4. Cost evaluation of sodium cooled FR

A method to evaluate construction cost of JSFR is developed. The method is revised based on that of construction-cost evaluation of DFBR which was used in the former joint study by utilities.

Two types of cost are classified based on the modified NUS codes of account: the cost of a sodium cooled FR facilities and equipment (direct cost) and the cost of miscellaneous expenses related to construction (indirect cost). Each account item is further developed into related facilities and equipments. NUS code of account was originally arranged by Nuclear Utility Service in 1969 for the evaluation of economics of LWRs, while the modified NUS code is a modified version of the original NUS code for the evaluation of FRs. The total plant construction cost is evaluated as the sum of all account items which are evaluated based on the formulae defined for each facility and equipment of the respective account items using the commodity data derived from the conceptual design of sodium cooled FR.

This cost evaluation formula is formulated as the product of a unit cost and the amount of materials for each facility and equipment, that is, basically formulated in the following form: construction cost of facilities and equipment = (amount of materials) × (unit cost).

The following four issues are presumed for the cost evaluation of sodium cooled FR: (1) the demand for resources used for the calculation of the interest during the construction period is to be raised fully on loan basis. The total demand is given as the sum of the direct cost and the indirect cost (excluding the interest during the construction). The proposed project period based on the field work is used as the construction period; (2) the demand curve for the resources is to be represented by a pattern curve used in the OECD/NEA evaluation, where the interest rate of 2% is used; (3) the owner's expense is to be 10% of the total construction cost (the sum of the direct cost and the indirect cost, excluding the interest during the construction period and the owner's expense); (4) the plant to be constructed is a twin plant and is assumed to replace a former water cooled reactor. The expenses of the land and the civil work for the accommodations already existed at the site, such as the harbor facilities not directly related to the building construction, are not included.

The value of 200 000 yen/kWe is set as a target for the construction cost of a sodium cooled FR. This value comes from that of the future construction cost of LWR for a first of a kind plant including the interest during construction. And the value of $1000/kWe in overnight cost with number of a kind corresponds to the above 200 000 yen/kWe.

The outcome of the construction cost evaluation shows that a large sodium cooled FR has the most promising capability of reducing the construction cost to 90% of the target, taking a full advantage of the scale merit.

The features and the commodity of a large sodium cooled FR and a same scale future water cooled reactor (APWR) are compared as shown in Table 4. From this table, the following three issues

Table 4
Comparison with a LWR

	Sodium cooled FR	LWR (APWR)
Electricity output (MWe)	1500	1530
Number of primary loops	2	4
Weights of the R/V (ton)	465	590
Weights of the IHX (ton)	520 (2 units)	–
Weights of the SG (ton)	1230 (2 units)	1760 (4 units)
Total (ton)	2215	2350
Volume of R/B	13×10^4 m^3 (round)	36×10^4 m^3 (round)

come: (1) Compared with the high temperature and the low pressure of a sodium cooled FR (550 °C/1.5 atg at reactor outlet), an APWR shows the lower temperature and the higher pressure characteristics (325 °C/160 atg). The plant thermal efficiency of a sodium cooled FR is of 42% which is higher than that of an APWR of 35%. (2) The reactor structure of a sodium cooled FR can be composed of thinner vessel plates, due to the lower plant pressure, which contributes to the reduction of construction commodity. (3) The cooling system of a large sodium cooled FR is presumed to be composed of 2 loops (2 intermediate heat exchangers and 2 steam generators), while a same scale APWR is composed of 4 loops (4 steam generators), which lead to nearly the same amount of total commodity of the cooling system. Furthermore, (4) the decay heat removal system of a sodium cooled reactor is presumed to be composed of 3 loops with full natural circulation heat removal capability, while that of an APWR is composed of lots of miscellaneous equipments related to the ECCS.

The result of our cost evaluation shows that JSFR with many innovative technologies has cost competitiveness as comparing of a future LWR.

5. Conclusions

The economical competitiveness would be essential to a new energy source in order to use it in the situation that the conventional energy sources are widely used. To get the competitiveness, we apply many innovative technologies to design of sodium cooled FR.

The high chromium ferritic steel in place of an austenitic stainless steel makes it possible to realize the simpler design of a sodium cooled FR, which is performed in design of JSFR. Critical technologies for the integrated pump/IHX component, the control of flow dynamics in the upper plenum of RV and the large diameter piping system are examined by experiments which reveal a strong possibility of the component and the control methods, though R&D work is still needed. ISI and repair method are developed on the basis of the low pressure and reducing atmosphere in sodium. Seismic isolation technology proceeds to apply for sodium cooled FR.

The cost evaluation of sodium cooled FR has been carried out based on the above technologies under the condition that the safety should be the first prerequisite. As a result, a sodium cooled FR can achieve the construction cost target to be competitive enough with a future LWR.

Acknowledgements

We are pleased to acknowledge providing a draft text of the section: Dr Aoto, Dr Chikazawa, Mr Fujii, Mr Hayafune, Mr Hishida, Dr Kasahara, Mr Kisohara, Mr Kitamura, Dr Morishita and Mr Takahashi of JAEA; Mr Ikeda, Mr Saigusa and Mr Uchida of JAPC. We are grateful to Dr Tôyama for a critical reading of the manuscript.

We should like to express our grateful thanks to Mitsubishi Heavy Industries, Ltd. who extended us their kind assistance.

A design activity except experimental activity was performed under collaboration between JAEA and JAPC together with Japanese electric companies. A part in Sections 2.3.1.5 and 2.3.1.6 in this paper was conducted by the JAEA and JAPC for research and development program of developing 'elevated temperature structural design guide for commercialized fast reactor' and 'three dimensional seismic isolation technology' on a contract basis with the METI. A part in Section 3 in this paper, especially, analyses and evaluation of the effect of contents of Tungsten and Molybdenum to the material properties was conducted under the financial support by the Ministry of Economy, Trade and Industry (METI) of Japanese government.

References

[1] M. Ando et al., Feasibility study on commercialized fast reactor cycle systems in Japan (II), 2005.
[2] Y. Shimakawa et al., Nucl. Technol. 140 (2002) 1.

[3] T. Fujii et al., ICONE13, Beijing, China, May, 2005, p. 16.
[4] T. Nakamura et al., in: Symposium on Flow-induced Vibration 2005, ASME Pressure Vessel and Piping Conference, Denver, Colorado, 17–21 July, 2005.
[5] T. Shiraishi et al., J. Fluid Eng. (2006) 1063.
[6] N. Kimura et al., NURETH-10, Seoul, Korea, October, 2003, p. 5.
[7] N. Kimura et al., NTHAS4, Sapporo, Japan, 28 November–1 December, 2004.
[8] Y. Eguchi et al., Nucl. Eng. Des. 146 (1994) 373.
[9] N. Sawa et. al., in: Proceedings of GLOBAL 2005, 2005.
[10] K. Iida et al., Construction codes for prototype FBR MONJU, NED 98, 1987, p. 283.
[11] ASME, Background of the ASME Boiler and Pressure Vessel Code for Design of Elevated Temperature Class 1 Components in Sec. III, New York, 1974.
[12] N. Kawasaki et al., Recent design improvements of elevated temperature structural design guide for DFBR in Japan, SMiRT15, Div. F, F04/4, 1999.
[13] N. Kasahara et al., Recent developments for fast reactor structural design standard (FDS), SMiRT 18, 2005, p. 1131.
[14] Y. Tanaka et al., ASME, PVP2004, PVP, vol. 472, 2004, p. 53.
[15] N. Kasahara, Masakazu Jinbo, Hiromi Hosogai, Mitigation method of thermal transient stress by thermal hydraulic-structure total analysis, SMiRT17, 2003, F03-1.
[16] N. Kasahara, H. Takasho, ASME, PVP, vol. 443-1, 2002, p. 25.
[17] N. Kimura et al., in: Proceedings of 2003 Annual Meeting of AESJ, J42, Sasebo, Japan, 2003.
[18] K. Takahashi et al., A development of three-dimensional seismic isolation for advanced reactor systems in Japan, 18th SMiRT, 2005, p. 3371.
[19] N. Kisohara et al., in: Proceedings of FR'91 Kyoto, Japan, 1991.
[20] N. Kisohara et.al., Flow and temperature distributions evaluation on sodium heated large sized straight double-wall-tubes steam generator, ICAPP '06, 2006.
[21] M. Konomura et al., JAEA-Research 2006-042, 2006, p. 517 (in Japanese).
[22] M. Fujita, in: World Hydrogen Energy Conference, 28PL-02, Yokohama Japan, 2004.
[23] Y. Chikazawa, T. Hori, M. Konomura, S. Uchida, Y. Tsuchiyama, in: 15th World Hydrogen Energy Conference, 30J-08, Yokohama Japan, 2004.
[24] T. Nakagiri, K. Aoto, T. Hoshiva, in: 15th World Hydrogen Energy Conference, 30J-07, Yokohama Japan, 2004.
[25] G.E. Beghi, Int. J. Hydrogen Energ. 4 (1994).
[26] Y. Chikazawa, T. Hori, M. Konomura, S. Uchida, Y. Tsuchiyama, Conceptual design of hydrogen production plant with thermochemical and electrolytic hybrid cycle using a sodium cooled reactor, ICAPP '05, Seoul, Korea No. 5084, 2005.
[27] M. Shiga et al., ISIJ 76 (7) (1990) 1092.
[28] T. Fujita, in: Proceedings of the 3rd International Charles Parsons Turbine Conference, Newcastle, 1995.
[29] T. Wakai et al., in: Proceedings of the 10th MPA seminar, MPA Stuttgart, 2004, p. 28-1.